Online Trajectory Scaling for Manipulators Subject to High-Order Kinematic and Dynamic Constraints

Corrado Guarino Lo Bianco and Oscar Gerelli

***Abstract*—Robotic manipulators are usually driven by means of minimum-time trajectories. Unfortunately, such trajectories strongly solicit the actuators whose dynamic limits could be easily exceeded. Therefore, kinematic and/or dynamic constraints are commonly considered for offline planning. Nevertheless, during actual operations, dynamic limits could be violated because of model uncertainties and measurement noise, thus causing performance losses. In order to fulfill the given bounds with certainty, planned trajectories are typically online scaled, by accounting for generalized force (GF) constraints. The resulting command signal is typically discontinuous; therefore, the system mechanics are unnecessarily solicited, and nonmodeled dynamics are excited. Moreover, in the case of systems that admit limited derivatives for GFs, tracking accuracy worsens. To prevent possible problems that derive from GF discontinuities, this paper proposes an online trajectory scaling approach that accounts for the simultaneous existence of joint constraints on GFs and their derivatives. At the same time, it is able to manage bounds on joint velocities, accelerations, and jerks.**

***Index Terms*—Bounded dynamics, bounded kinematics, manipulator dynamics, robot motion, trajectory scaling.**

I. Introduction

The productivity of industrial processes is clearly related to the time required to accomplish the assigned tasks. Therefore, when robotic manipulators are involved, users ask for very demanding trajectories, which possibly exceed the manipulators limits and cause tracking losses. For this reason, kinematics limits are normally considered during the trajectory planning phase, e.g., by bounding joint velocities, accelerations, and jerks. When possible, generalized force (GF) constraints are also considered. Typically, existing bounds are taken into account by means of offline optimization algorithms that minimize traveling times while simultaneously handling explicit kinematic and/or dynamic constraints. In some works, trajectories are planned as a whole [1], while in others, the path-velocity decomposition scheme [2] is adopted. In this latter framework, initial results for nonredundant manipulators have been proposed in [3], where a scaling factor was introduced to guarantee the feasibility of a planned trajectory. This approach has been subsequently extended to robots in cooperative tasks [4] and for manipulators with elastic joints [5]. Alternative approaches, which are not based on standard optimization algorithms, were proposed in the two independent works [6], [7].

Mentioned offline methods are characterized by a couple of drawbacks. First, they do not foresee the effects of external disturbances that act on real manipulators, and as such, they do not manage model uncertainties. As a consequence, disturbances and modeling errors are subsequently compensated by the feedback controller that generates GFs that, being different from those originally planned, could saturate the actuators. Second, they cannot be used in applications that require an on-the-fly planning, such as, for example, the tracking of a moving object whose trajectory is not known *a priori*.

The first kind of problems can still be handled by using offline strategies like that proposed in [8]: The real system is investigated in advance by the execution of test trajectories that are subsequently used to generate almost time-optimal transients that robustly avoid saturations. The situation becomes more complex when trajectories are modified on-the-fly: because of the lack of time, their feasibility cannot be guaranteed.

Online approaches have been proposed to handle these situations: starting from any desired trajectory, which could also be unfeasible, online methods scale it in order to satisfy the system constraints. Proposals have appeared in [9] and [10] for manipulators subject to kinematic constraints, in [11]–[17] for systems subject to torque limits, while in [18], a robust online extension of [3] has been described.

In recent papers [19], [20], the bounding problem has been extended by the consideration of the existence of constraints on the time derivatives of GFs. Indeed, GF derivatives (GFDs) are evidently bounded in many systems that are characterized by slow dynamics, like hydraulically actuated systems; therefore, if bounds are not taken into account, controller performances degenerate. Moreover, even when actuators are able to handle large GFDs, it is better to bound them since discontinuities on GFs solicit the system mechanics and excite undesired dynamics because of gears backlashes and elasticity. GFs discontinuities are common to the aforementioned online strategies, since they typically downscale trajectories while simultaneously satisfying an optimality criterion: An immediate consequence is that GFs assume bang–bang shapes. That is what happens in [17], for example, where planned trajectories, which are sometimes abandoned to preserve GFs limits, are newly hanged in minimum time when dynamic bounds no longer represent a problem. For this purpose, discontinuous GFs are used.

To preserve optimality and avoid GFs discontinuities, in this study, a novel online trajectory scaling system is proposed, which improves the results achieved in [17] by also considering constraints on GFDs. Early results that are proposed in [21] and [22] are here improved with the help of the novel filter devised in [23]. The new filter online scales trajectories by simultaneously accounting for the existence of constraints on GFs and GFDs, as well as on joint velocities, accelerations, and jerks. It is worth noticing that, in realistic scenarios, only a subset of such constraints are normally considered: For example, trajectories could be scaled by only considering bounds on velocities, GFs, and GFDs or, in the case of inadequate knowledge of the manipulator dynamics, it could be possible to consider an alternative problem where only kinematic constraints are involved, owing to the correlation that exists between accelerations and GFs, as well as between jerks and GFDs. As a further step forward with respect to [21] and [22], the velocity profile that is used to move along the planned path is directly defined in the time domain. This choice, which is also adopted in [15]–[17], is the reason of two important improvements: The time law is generated by means of standard planning methods and, more important, time delays that are accumulated because of saturations are recovered as soon as those limitations cease.

The paper is organized as follows. In Section II, the trajectory scaling problem is formulated. Some feasibility considerations that concern the trajectory scaling problem are drawn in Section III. The control strategy and the method that are used for the online conversion of the joint bounds into equivalent limits for the longitudinal time law

Manuscript received October 20, 2010; revised March 14, 2011; accepted July 4, 2011. Date of publication August 18, 2011; date of current version December 8, 2011. This paper was recommended for publication by Associate Editor D. Lee and Editor G. Oriolo upon evaluation of the reviewers' comments. This work is supported in part by the Ateneo Italo Tedesco in the framework of a Vigoni project.

The authors are with the Department of Information Engineering, University of Parma, I-43100 Parma, Italy (e-mail: guarino@ce.unipr.it; gerelli@ce.unipr.it).

Color versions of one or more of the figures in this paper are available online at http://ieeexplore.ieee.org.

Digital Object Identifier 10.1109/TRO.2011.2162268

are described in Section IV. The overall control strategy is tested in Section V by means of example cases. Section VI concludes this paper.

NOTATION

The elements of any generic vector $\mathbf{t} \in \mathbb{R}^n$ are indicated as t_k, where $k = 1, 2, \ldots, n$. $\mathscr{C}^i$ indicates the set of functions that are continuous until the ith derivative, while $\mathscr{C}_p$ indicates the set of piecewise continuous functions. Overlined and underlined symbols, respectively, indicate the upper bound and the lower bound of a variable, e.g., $\overline{\dot{q}}_k$ is the upper bound of the kth joint velocity, while $\underline{\dot{q}}_k$ is the corresponding lower bound. Along this paper, upper and lower bounds are always supposed to be known. They can also be time varying.

II. TRAJECTORY SCALING PROBLEM

Let us define a parametric curve in the joint space by means of a vector function $\mathbf{f}(u)$ that is defined as follows:

$$\begin{aligned} \mathbf{f} : [0, u_f] &\rightarrow \mathbb{R}^n \\ u &\rightarrow \mathbf{q}_d := \mathbf{f}(u) \end{aligned} \tag{1}$$

where u is the scalar that is used to parameterize the curve, u_f is its final value, and n is the number of independent joints. The curve must be planned such that $\mathbf{f}(u)''' \in \mathscr{C}_p([0, u_f])$ and $\mathbf{f}(u)' \neq 0 \; \forall u \in [0, u_f]$, where the superscript $'$ indicates a differentiation with respect to u, e.g., $\mathbf{f}(u)' = [d\mathbf{f}(u)]/(du)$, while as usual, dots will be used in the following to indicate time derivatives, e.g., $\dot{u}(t) = [du(t)]/(dt)$.

In the same way, it is possible to define a monotonically increasing time law to move along the curve

$$\begin{aligned} u : [0, t_f] &\rightarrow [0, u_f] \\ t &\rightarrow u_d := u(t) \end{aligned} \tag{2}$$

where t_f is the total traveling time. Reasonably, $\dot{u}_d(t) > 0$ for any $t \in (0, t_f)$. This implies that motion cannot be inverted or stopped in any point along the path. The overall robot trajectory is obtained by the combination of (1) and (2): $\mathbf{q}_d = \mathbf{f}[u(t)]$. By taking into account the chain differentiation rule, the trajectory time derivatives are

$$\dot{\mathbf{q}}_d(u, \dot{u}) = \mathbf{f}(u)' \dot{u} \tag{3}$$

$$\ddot{\mathbf{q}}_d(u, \dot{u}, \ddot{u}) = \mathbf{f}(u)'' \dot{u}^2 + \mathbf{f}(u)' \ddot{u} \tag{4}$$

$$\dddot{\mathbf{q}}_d(u, \dot{u}, \ddot{u}, \dddot{u}) = \mathbf{f}(u)''' \dot{u}^3 + 3\mathbf{f}(u)'' \dot{u}\ddot{u} + \mathbf{f}(u)' \dddot{u} \, . \tag{5}$$

Problem 1: Given a trajectory, which is represented according to the path-velocity decomposition, its longitudinal time law must be automatically scaled such that path tracking is not lost even when kinematic and/or dynamic saturations occur.

Practically, this allows trajectory tracking to be lost when limits are reached, to try to preserve an accurate path tracking. It is relevant to point out which constraints can be handled by means of the proposed approach. Usually [11], trajectory scaling only considers GF constraints, i.e., the trajectory is online modified such that, at any time, GF τ_k of the kth joint is bounded between assigned limits, i.e.,

$$\underline{\tau}_k \leq \tau_k \leq \overline{\tau}_k, \quad k = 1, 2, \ldots, n \, . \tag{6}$$

In this paper, the problem is extended in order to guarantee that (6) is fulfilled together with other constraints. For example, still remaining in a dynamic context, for the reasons highlighted in Section I, it could be important to limit maximum GFDs $\dot{\tau}_k$. Formally, this result is achieved by guaranteeing that the following inequalities are simultaneously satisfied:

$$\underline{\dot{\tau}}_k \leq \dot{\tau}_k \leq \overline{\dot{\tau}}_k \, , \quad k = 1, 2, \ldots, n \, . \tag{7}$$

Furthermore, kinematic constraints on joint velocities $\dot{q}_k$, accelerations $\ddot{q}_k$, and jerks $\dddot{q}_k$ are considered as well, by imposing ($k = 1, 2, \ldots, n$)

$$\underline{\dot{q}}_k \leq \dot{q}_k \leq \overline{\dot{q}}_k \tag{8}$$

$$\underline{\ddot{q}}_k \leq \ddot{q}_k \leq \overline{\ddot{q}}_k \tag{9}$$

$$\underline{\dddot{q}}_k \leq \dddot{q}_k \leq \overline{\dddot{q}}_k \, . \tag{10}$$

It is interesting to notice that in order to meet kinematic bounds, both $\mathbf{f}(u)$ and $u(t)$ must fulfill some requirements.

Proposition 1: Any trajectory that is planned according to the path-velocity decomposition scheme can be followed with bounded joint velocities, accelerations, and jerks iff $\mathbf{f}(u)''' \in \mathscr{C}_p([0, u_f])$ and $\dddot{u}(t) \in \mathscr{C}_p([0, t_f])$.

Proof: It immediately descends from (3)–(5).

Sufficiency: If $\mathbf{f}(u)''' \in \mathscr{C}_p([0, u_f])$ and $\dddot{u}(t) \in \mathscr{C}_p([0, t_f])$, then, necessarily, $\mathbf{f}(u) \in \mathscr{C}^2([0, u_f])$ and $u(t) \in \mathscr{C}^2([0, t_f])$. This, in turn implies, owing to (3)–(5), that $\dddot{\mathbf{q}}_d \in \mathscr{C}_p([0, t_f])$, while $\mathbf{q}_d \in \mathscr{C}^2([0, t_f])$, i.e., joints velocities, accelerations, and jerks are bounded.

Necessity: Let us suppose that $\dddot{\mathbf{q}}_d$ is bounded but $\mathbf{f}(u)''' \notin \mathscr{C}_p([0, u_f])$, or $\dddot{u}(t) \notin \mathscr{C}_p([0, t_f])$. This is clearly impossible because of (5). ■

Remark 1: An immediate consequence of *Proposition* 1 is that, owing to kinematic bounds, $\mathbf{f}(u)'$, and $\mathbf{f}(u)''$, $\dot{u}(t)$ and $\ddot{u}(t)$ must be continuous functions. This is a general property which applies independently from the adopted control strategy.

The problem that is considered in this paper accounts for the simultaneous existence of constraints (6)–(10). It is worth remarking that, as asserted in Section I, the same approach can handle problems where such constraints are not simultaneously imposed.

III. SOME FEASIBILITY CONSIDERATIONS

Given a manipulator and a trajectory $\mathbf{q}_d = \mathbf{f}[u(t)]$, we want to verify if this trajectory is feasible with respect to (6) and (7).

To this purpose, closed-form equations are compulsory for both GFs and GFDs. As usual, GFs can be evaluated with the classic inverse dynamics equation

$$\boldsymbol{\tau} = \mathbf{H}(\mathbf{q})\, \ddot{\mathbf{q}} + \mathbf{C}(\mathbf{q}, \dot{\mathbf{q}})\dot{\mathbf{q}} + \mathbf{g}(\mathbf{q}) + \mathbf{v}(\mathbf{q}, \dot{\mathbf{q}}) \, . \tag{11}$$

Here, $\mathbf{q}, \dot{\mathbf{q}}, \ddot{\mathbf{q}} \in \mathbb{R}^n$ indicate the joint variables and their first and second time derivatives, $\mathbf{H}(\mathbf{q}) \in \mathbb{R}^{n \times n}$ is the symmetric and definite positive inertia matrix, $\mathbf{C}(\mathbf{q}, \dot{\mathbf{q}}) \in \mathbb{R}^{n \times n}$ is the matrix of centripetal and Coriolis terms, $\mathbf{g} \in \mathbb{R}^n$ is the vector of the gravity forces, and $\mathbf{v}(\mathbf{q}, \dot{\mathbf{q}}) \in \mathbb{R}^n$ is the vector of the friction forces.

The time derivative of (11) can be easily evaluated [22] and posed into the following compact form:

$$\begin{aligned} \dot{\boldsymbol{\tau}} = \dot{\mathbf{H}}(\mathbf{q}, \dot{\mathbf{q}})\, \ddot{\mathbf{q}} + \mathbf{H}(\mathbf{q})\dddot{\mathbf{q}} + \mathbf{D}(\mathbf{q}, \dot{\mathbf{q}})\, \dot{\mathbf{q}} + 2\mathbf{C}(\mathbf{q}, \dot{\mathbf{q}})\, \ddot{\mathbf{q}} \\ + \mathbf{L}(\mathbf{q}, \dot{\mathbf{q}})\, \dot{\mathbf{q}} + \mathbf{E}(\mathbf{q}, \dot{\mathbf{q}})\, \ddot{\mathbf{q}} \, . \end{aligned} \tag{12}$$

The first two terms represent the components of the GFD which depend on the system inertia. In the same way, the second two terms derive from the Coriolis and the centripetal forces, while the last two terms refer to the gravity and the friction effects.

Because of (1)–(5), (11) and (12) can be expressed as functions of u and its derivatives

$$\boldsymbol{\tau}(u,\dot{u},\ddot{u}) = \mathbf{a}_1(u)\ddot{u} + \mathbf{a}_2(u,\dot{u}) \tag{13}$$

$$\dot{\boldsymbol{\tau}}(u,\dot{u},\ddot{u},\dddot{u}) = \mathbf{b}_1(u)\dddot{u} + \mathbf{b}_2(u,\dot{u},\ddot{u}) \tag{14}$$

where

$$\mathbf{a}_1(u) = \mathbf{b}_1(u) := \mathbf{H}[\mathbf{q}_d(u)]\mathbf{f}(u)' \tag{15}$$

$$\begin{aligned}\mathbf{a}_2(u,\dot{u}) := {} & \mathbf{H}[\mathbf{q}_d(u)]\mathbf{f}(u)''\dot{u}^2 \\ & + \mathbf{C}[\mathbf{q}_d(u),\dot{\mathbf{q}}_d(u,\dot{u})]\dot{\mathbf{q}}_d(u,\dot{u}) \\ & + \mathbf{v}[\mathbf{q}_d(u),\dot{\mathbf{q}}_d(u,\dot{u})] + \mathbf{g}[\mathbf{q}_d(u)]\end{aligned} \tag{16}$$

$$\begin{aligned}\mathbf{b}_2(u,\dot{u},\ddot{u}) := {} & \mathbf{H}[\mathbf{q}_d(u)][\mathbf{f}(u)'''\dot{u}^3 + 3\mathbf{f}(u)''\dot{u}\ddot{u}] \\ & + \dot{\mathbf{H}}[\mathbf{q}_d(u),\dot{\mathbf{q}}_d(u,\dot{u})]\,\dot{\mathbf{q}}_d(u,\dot{u},\ddot{u}) \\ & + \mathbf{D}[\mathbf{q}_d(u),\dot{\mathbf{q}}_d(u,\dot{u})]\,\dot{\mathbf{q}}_d(u,\dot{u}) \\ & + 2\mathbf{C}[\mathbf{q}_d(u),\dot{\mathbf{q}}_d(u,\dot{u})]\,\ddot{\mathbf{q}}_d(u,\dot{u},\ddot{u}) \\ & + \mathbf{L}[\mathbf{q}_d(u),\dot{\mathbf{q}}_d(u,\dot{u})]\,\dot{\mathbf{q}}_d(u,\dot{u}) \\ & + \mathbf{E}[\mathbf{q}_d(u),\dot{\mathbf{q}}_d(u,\dot{u})]\,\ddot{\mathbf{q}}_d(u,\dot{u},\ddot{u})\end{aligned} \tag{17}$$

and where $\mathbf{a}_1(u) = [a_{1,1}\ a_{1,2}\ \cdots\ a_{1,n}]^T \in \mathbb{R}^n$, $\mathbf{a}_2(u,\dot{u}) = [a_{2,1}\ a_{2,2}\ \cdots\ a_{2,n}]^T \in \mathbb{R}^n$, $\mathbf{b}_1(u) = [b_{1,1}\ b_{1,2}\ \cdots\ b_{1,n}]^T \in \mathbb{R}^n$, and $\mathbf{b}_2(u,\dot{u},\ddot{u}) = [b_{2,1}\ b_{2,2}\ \cdots\ b_{2,n}]^T \in \mathbb{R}^n$.

Like in the case of kinematic constraints, bounds on the GFs and the GFDs impose some requirements on the characteristics of $\mathbf{f}(u)$ and of $u(t)$.

Proposition 2: Any trajectory that is planned according to the path-velocity decomposition scheme can be followed with bounded GFs and GFDs iff $\mathbf{f}(u)''' \in \mathscr{C}_p([0,u_f])$ and $\dddot{u}(t) \in \mathscr{C}_p([0,t_f])$.

Proof: The proof is a direct consequence of (13)–(17) and of (3)–(5). The same reasonings used for the demonstration of *Proposition* 1 apply. The demonstration is omitted for conciseness. ■

Remark 2: Boundedness of $\boldsymbol{\tau}$ and $\dot{\boldsymbol{\tau}}$, because of *Proposition* 2, impose on the curve geometry and on the longitudinal time law the same constraints that are described in *Remark 1*.

Owing to (13) and (14), constraints (6) and (7) are fulfilled if the following inequalities are simultaneously satisfied:

$$\underline{\tau}_k \le a_{1,k}(u)\ddot{u} + a_{2,k}(u,\dot{u}) \le \overline{\tau}_k \tag{18}$$

$$\underline{\dot{\tau}}_k \le b_{1,k}(u)\dddot{u} + b_{2,k}(u,\dot{u},\ddot{u}) \le \overline{\dot{\tau}}_k\ . \tag{19}$$

By means of (18) and (19), it is possible to define a feasible zones in the $[u,\dot{u},\ddot{u}]$-space.

For torque constraint (18), the problem has been widely investigated in the past [3], [6], [7], [11], both for offline and online approaches. In particular, the feasible zone in the $(u,\dot{u})$-plane is given by the area where, for any pair u, $\dot{u}$, there exists at least one value $\ddot{u}$ which fulfills (18): Any trajectory that is completely contained in such region is feasible with respect to the GF constraint (see, e.g., area $\mathscr{B}$ in Fig. 1). If also GFD constraints are addressed, the feasible zone becomes 3-D and coincides with the volume where, for any triplet u, $\dot{u}$, and $\ddot{u}$, there exists at least one value $\dddot{u}$ that fulfills (19). Fig. 1 shows feasible volume $\mathscr{A}$ for the manipulator that is proposed in Section V. Upper bounds on $\dot{u}$ coincide for $\mathscr{A}$ and $\mathscr{B}$; therefore, it is possible to summarize that any feasible longitudinal time-law $u(t)$ must necessarily be entirely constrained in $\mathscr{A}$—and, consequently, in $\mathscr{B}$—and formulate the following definition of feasibility.

Definition 1: Given a manipulator (11) and (12), a curve $\mathbf{f}(u)$, and a time law $u(t)$, the resulting trajectory $\mathbf{f}[u(t)]$ is feasible with respect to the GF and GFD constraints iff curve $[u(t),\dot{u}(t),\ddot{u}(t)]$ belongs to $\mathscr{A}$ for any $t \in [0,t_f]$.

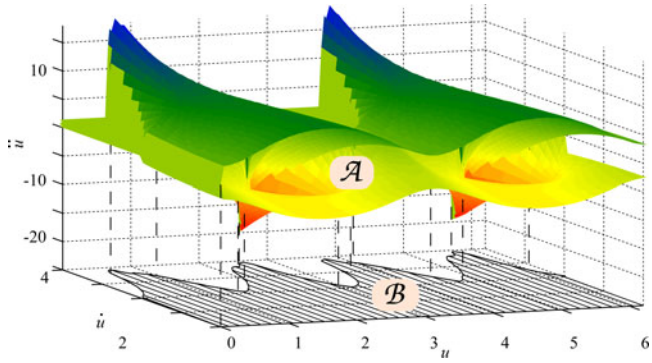

Fig. 1. Example of admissible regions $\mathscr{A}$ and $\mathscr{B}$ corresponding to the manipulator that is proposed in Section V.

Obviously, if GF and GFD constraints are not taken into account, there is no certainty that the planned trajectory will be completely contained in $\mathscr{A}$, but even when they are considered, feasibility is not guaranteed. This assertion can be easily justified. Feasible region $\mathscr{A}$ can only be evaluated on the basis of an estimated manipulator model. This implies that $\mathscr{A}$ is a theoretical feasible region which can differ from the actual one because of model uncertainties. This mismatching can be very critical if, e.g., optimal trajectories have been computed by an offline algorithm that minimizes traveling time subject to GF and GFD constraints. Indeed, it is known that resulting curves constantly lie on the boundaries of the theoretical feasible zone; therefore, they can easily violate the bounds of actual $\mathscr{A}$.

Every time actual $\mathscr{A}$ is abandoned, path tracking is lost. For this reason, online algorithms that are able to online estimate the actual bounds of $\mathscr{A}$ and to force the system inside such limits must be devised.

Kinematic constraints also affect the shape of $\mathscr{A}$. Nevertheless, they are less critical than dynamic constraints: In the next section, it will be shown that kinematic constraints only depend on $\mathbf{f}(u)$, which, differently from the manipulator model, is perfectly known.

IV. Trajectory Scaling Approach

The trajectory scaling approach that is described in this paper is able to overcome the problems that are mentioned in Section III. The proposed implementation is suited to be used both with feedforward controllers with position and velocity feedback (FCPVs) and with inverse dynamics controllers (IDCs). For conciseness, the discussion will only involve IDCs, but obtained results can be easily extended to FCPVs according to the approach that is proposed in [21]. The dynamic equation of an IDC is

$$\begin{aligned}\boldsymbol{\tau} = {} & \widehat{\mathbf{H}}(\mathbf{q})\,\ddot{\mathbf{q}}_d + \widehat{\mathbf{C}}(\mathbf{q},\dot{\mathbf{q}})\dot{\mathbf{q}} + \widehat{\mathbf{g}}(\mathbf{q}) + \widehat{\mathbf{v}}(\mathbf{q},\dot{\mathbf{q}}) \\ & + \mathbf{k}_p^T\,\mathbf{e} + \mathbf{k}_v^T\,\dot{\mathbf{e}}\end{aligned} \tag{20}$$

where $\mathbf{k}_p, \mathbf{k}_v \in (\mathbb{R}^+)^n$ are the controller gain vectors, while $\mathbf{e} := \mathbf{q} - \mathbf{q}_d$, $\dot{\mathbf{e}} := \dot{\mathbf{q}} - \dot{\mathbf{q}}_d$ represent, respectively, the trajectory tracking error and its derivative. Symbol $\widehat{\ }$ points out that the controller is based on an estimate of the manipulator model.

Even when a trajectory is planned to be feasible with respect to (6), i.e., (18) is satisfied, feasibility can be lost because of the reasons that are discussed in Section III. The control scheme that is shown in Fig. 2 is suited to manage possible feasibility issues. The manipulator whose model accounts for kinematic and dynamic saturations is driven by means of an IDC. Reference trajectories are planned in the joint

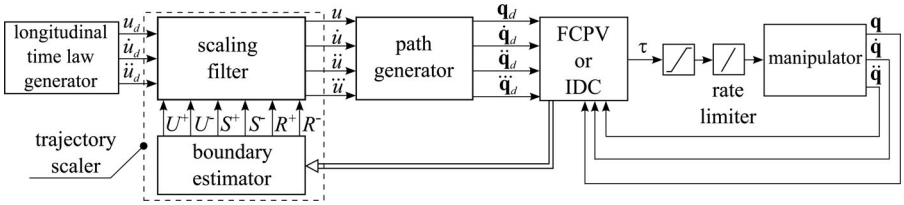

Fig. 2. Overall manipulator control scheme. The dashed box surrounds the automatic trajectory scaling system.

space according to the path-velocity decomposition paradigm: The path generator evaluates $\mathbf{q}_d$, $\dot{\mathbf{q}}_d$, $\ddot{\mathbf{q}}_d$, and $\dddot{\mathbf{q}}_d$ by means of (1), (3), (4), and (5) so that they are clearly function of the curvilinear coordinate u and its derivatives. Commonly, u and its derivatives, i.e., the longitudinal time law, are directly obtained by means of a scalar trajectory generator. In the modified control scheme that is proposed in this study, a trajectory scaler is posed between the time-law generator and the path generator. It is designed to online scale the reference time law in order to fulfill the assigned dynamic and/or kinematic constraints.

The trajectory scaler is composed of two blocks. The first converts kinematic and dynamic constraints into equivalent constraints for the longitudinal time law: Joint constraints are converted into upper and lower bounds for the longitudinal velocity, namely R^+ and R^-, for the longitudinal acceleration, namely S^+ and S^-, and for the longitudinal jerk, namely U^+ and U^-. All bounds are online evaluated and continuously change depending on the system status. The second block is a modified version of the nonlinear filter proposed in [23] and is used to scale the longitudinal time law in order to fulfill the converted constraints.

It is clearly important to understand how joint dynamic and kinematic constraints can be transformed into equivalent bounds for $u(t)$ and its derivatives. Regarding the GF and the GFD constraints, the conversion depends on the adopted controller.

Under the hypothesis that the manipulator is following path $\mathbf{f}(u)$, (20) can be rewritten, because of (4), as follows:

$$\boldsymbol{\tau}(u,\dot{u},\ddot{u};\mathbf{q},\dot{\mathbf{q}}) = \widehat{\mathbf{a}}_1(u;\mathbf{q})\ddot{u} + \widehat{\mathbf{a}}_2(u,\dot{u};\mathbf{q},\dot{\mathbf{q}}) \tag{21}$$

where

$$\widehat{\mathbf{a}}_1(u;\mathbf{q}) := \widehat{\mathbf{H}}(\mathbf{q})\,\mathbf{f}(u)' \tag{22}$$

$$\begin{aligned}\widehat{\mathbf{a}}_2(u,\dot{u};\mathbf{q},\dot{\mathbf{q}}) := {}& \widehat{\mathbf{H}}(\mathbf{q})\,\mathbf{f}(u)''\dot{u}^2 + \widehat{\mathbf{C}}(\mathbf{q},\dot{\mathbf{q}})\dot{\mathbf{q}} + \widehat{\mathbf{g}}(\mathbf{q}) + \widehat{\mathbf{v}}(\mathbf{q},\dot{\mathbf{q}}) \\ & + \mathbf{k}_p^T\,\mathbf{e} + \mathbf{k}_v^T\,\dot{\mathbf{e}}\end{aligned} \tag{23}$$

and where $\widehat{\mathbf{a}}_1(u;\mathbf{q}) = [\widehat{a}_{11}, \widehat{a}_{12}, \ldots, \widehat{a}_{1n}]^T$, and $\widehat{\mathbf{a}}_2(u,\dot{u};\mathbf{q},\dot{\mathbf{q}}) = [\widehat{a}_{21}, \widehat{a}_{22}, \ldots, \widehat{a}_{2n}]^T$.

Equation (21) is instrumental for converting constraints on GFs into equivalent bounds on $\ddot{u}$ according to the technique that was originally proposed in [11]. In particular, for the kth joint it is possible to write $\tau_k = \widehat{a}_{1k}\ddot{u} + \widehat{a}_{2k}$ so that, depending on the current values of $u, \dot{u}, \ddot{u}, \mathbf{q}$, and $\dot{\mathbf{q}}$, constraints (6) are satisfied if the following inequalities simultaneously hold:

$$\underline{\tau}_k \le \widehat{a}_{1k}\,\ddot{u} + \widehat{a}_{2k} \le \overline{\tau}_k, \quad k = 1,2,\ldots,n\,. \tag{24}$$

Since (21) is also used by the controller for the evaluation of $\boldsymbol{\tau}$, at any time $\widehat{\mathbf{a}}_1$ and $\widehat{\mathbf{a}}_2$ are both known, and consequently, they are immediately available for the online estimation of the admissible bounds on $\ddot{u}$ at no additional cost. More in detail, (24) implies that feasibility is guaranteed if $\ddot{u} \in \bigcap_{k=1}^{n}[\beta_k\ ,\alpha_k]$, with

$$\alpha_k = \begin{cases} \dfrac{\overline{\tau}_k - \widehat{a}_{2k}}{\widehat{a}_{1k}}, & \text{if } \widehat{a}_{1k} > 0 \\ \dfrac{\underline{\tau}_k - \widehat{a}_{2k}}{\widehat{a}_{1k}}, & \text{if } \widehat{a}_{1k} < 0 \\ \infty, & \text{if } \widehat{a}_{1k} = 0 \end{cases} \tag{25}$$

$$\beta_k = \begin{cases} \dfrac{\underline{\tau}_k - \widehat{a}_{2k}}{\widehat{a}_{1k}}, & \text{if } \widehat{a}_{1k} > 0 \\ \dfrac{\overline{\tau}_k - \widehat{a}_{2k}}{\widehat{a}_{1k}}, & \text{if } \widehat{a}_{1k} < 0 \\ -\infty, & \text{if } \widehat{a}_{1k} = 0. \end{cases} \tag{26}$$

As early anticipated, the scaling strategy that was originally proposed in [11] is improved in this study by accounting for the boundedness of the GFDs. GFDs for IDCs can be obtained by differentiating (20). The same manipulations that are considered while devising (12) lead to

$$\begin{aligned}\dot{\boldsymbol{\tau}} = {}& \dot{\widehat{\mathbf{H}}}(\mathbf{q},\dot{\mathbf{q}})\,\ddot{\mathbf{q}}_d + \widehat{\mathbf{H}}(\mathbf{q})\dddot{\mathbf{q}}_d + \widehat{\mathbf{D}}(\mathbf{q},\dot{\mathbf{q}})\,\dot{\mathbf{q}} + 2\widehat{\mathbf{C}}(\mathbf{q},\dot{\mathbf{q}})\,\ddot{\mathbf{q}} \\ & + \widehat{\mathbf{L}}(\mathbf{q},\dot{\mathbf{q}})\,\dot{\mathbf{q}} + \widehat{\mathbf{E}}(\mathbf{q},\dot{\mathbf{q}})\,\ddot{\mathbf{q}} + \mathbf{k}_p^T\,\dot{\mathbf{e}} + \mathbf{k}_v^T\,\ddot{\mathbf{e}}\,.\end{aligned} \tag{27}$$

In addition, this expression can be parameterized in function of the curvilinear coordinate u by means of (4) and (5), leading to

$$\dot{\boldsymbol{\tau}}(u,\dot{u},\ddot{u},\dddot{u};\mathbf{q},\dot{\mathbf{q}},\ddot{\mathbf{q}}) = \widehat{\mathbf{b}}_1(u;\mathbf{q})\dddot{u} + \widehat{\mathbf{b}}_2(u,\dot{u},\ddot{u};\mathbf{q},\dot{\mathbf{q}},\ddot{\mathbf{q}}) \tag{28}$$

where

$$\widehat{\mathbf{b}}_1(u;\mathbf{q}) = \widehat{\mathbf{a}}_1(u;\mathbf{q}) := \widehat{\mathbf{H}}(\mathbf{q})\,\mathbf{f}(u)' \tag{29}$$

$$\begin{aligned}\widehat{\mathbf{b}}_2(u,\dot{u},\ddot{u};\mathbf{q},\dot{\mathbf{q}},\ddot{\mathbf{q}}) := {}& \dot{\widehat{\mathbf{H}}}(\mathbf{q},\dot{\mathbf{q}})\,[\mathbf{f}(u)''\dot{u}^2 + \mathbf{f}(u)'\ddot{u}] \\ & + \widehat{\mathbf{H}}(\mathbf{q})\,[\mathbf{f}(u)'''\dot{u}^3 + 3\mathbf{f}(u)''\dot{u}\ddot{u}] \\ & + \widehat{\mathbf{D}}(\mathbf{q},\dot{\mathbf{q}})\,\dot{\mathbf{q}} + 2\widehat{\mathbf{C}}(\mathbf{q},\dot{\mathbf{q}})\,\ddot{\mathbf{q}} + \widehat{\mathbf{L}}(\mathbf{q},\dot{\mathbf{q}})\,\dot{\mathbf{q}} \\ & + \widehat{\mathbf{E}}(\mathbf{q},\dot{\mathbf{q}})\,\ddot{\mathbf{q}} + \mathbf{k}_p^T\,\dot{\mathbf{e}} + \mathbf{k}_v^T\,\ddot{\mathbf{e}}\,.\end{aligned} \tag{30}$$

Thus, the requirements on GFDs are satisfied if the following inequalities are simultaneously fulfilled:

$$\dot{\underline{\tau}}_k \le \widehat{b}_{1k}\dddot{u} + \widehat{b}_{2k} \le \dot{\overline{\tau}}_k, \quad k = 1,2,\ldots,n\,. \tag{31}$$

In the case of GFDs, some additional computational burden is required, since more terms have to be evaluated online. Term $\widehat{\mathbf{b}}_1(u;\mathbf{q}) = \widehat{\mathbf{a}}_1(u;\mathbf{q})$ is already known since it is the same that appears in (22), but the online evaluation of $\widehat{\mathbf{b}}_2(u,\dot{u},\ddot{u};\mathbf{q},\dot{\mathbf{q}},\ddot{\mathbf{q}})$ could be time consuming. For this reason, an efficient method for the online evaluation of $\widehat{\mathbf{b}}_2(u,\dot{u},\ddot{u};\mathbf{q},\dot{\mathbf{q}},\ddot{\mathbf{q}})$ was proposed in [22]. It is based on an extended iterative Newton–Euler algorithm devised in [24], which is able to evaluate (12) with a computational burden comparable with that required by standard Newton–Euler algorithms for the evaluation of (11). Matrix $\dot{\widehat{\mathbf{H}}}(\mathbf{q},\dot{\mathbf{q}})$, which is essential for the evaluation of $\widehat{\mathbf{b}}_2$, can be obtained by means of the efficient algorithm that is proposed in [22]. Since $\widehat{\mathbf{b}}_1$ and

$\widehat{\mathbf{b}}_2$ can be evaluated online, from now on, both terms are assumed to be known: They will be used for the conversion of the GFD constraints into equivalent bounds on the longitudinal jerk $\dddot{u}$. More precisely, by virtue of (31), feasibility is achieved if $\dddot{u} \in \bigcap_{k=1}^{n}[\delta_k\ , \gamma_k]$, with

$$\gamma_k = \begin{cases} \dfrac{\dot{\overline{\tau}}_k - \widehat{b}_{2k}}{\widehat{b}_{1k}}, & \text{if } \widehat{b}_{1k} > 0 \\ \dfrac{\dot{\underline{\tau}}_k - \widehat{b}_{2k}}{\widehat{b}_{1k}}, & \text{if } \widehat{b}_{1k} < 0 \\ \infty, & \text{if } \widehat{b}_{1k} = 0 \end{cases} \tag{32}$$

$$\delta_k = \begin{cases} \dfrac{\dot{\underline{\tau}}_k - \widehat{b}_{2k}}{\widehat{b}_{1k}}, & \text{if } \widehat{b}_{1k} > 0 \\ \dfrac{\dot{\overline{\tau}}_k - \widehat{b}_{2k}}{\widehat{b}_{1k}}, & \text{if } \widehat{b}_{1k} < 0 \\ -\infty, & \text{if } \widehat{b}_{1k} = 0. \end{cases} \tag{33}$$

Additional restrictions must be considered in order to constraint joints jerks, accelerations, and velocities between assigned bounds. Assuming that the manipulator is currently tracking the path, it is possible to assert that $\mathbf{q} = \mathbf{q}_d$ so that for each joint $k = 1, 2, \ldots, n$ constraints (8)–(10) can be rewritten, because of (3)–(5), as follows:

$$\dot{\underline{q}}_k \leq f_k(u)'\dot{u} \leq \dot{\overline{q}}_k \tag{34}$$

$$\ddot{\underline{q}}_k \leq f_k(u)''\dot{u}^2 + f_k(u)'\ddot{u} \leq \ddot{\overline{q}}_k \tag{35}$$

$$\dddot{\underline{q}}_k \leq f_k(u)'''\dot{u}^3 + 3f_k(u)''\dot{u}\ddot{u} + f_k(u)'\dddot{u} \leq \dddot{\overline{q}}_k\ . \tag{36}$$

It is then possible to convert such bounds into equivalent constraints on $\dot{u}$, on $\ddot{u}$, and on $\dddot{u}$. In particular, (34) is fulfilled if the longitudinal velocity is bounded according to the following expression $\dot{u} \in \bigcap_{k=1}^{n}[0\ , \eta_k]$, where

$$\eta_k = \begin{cases} \dfrac{\dot{\overline{q}}_k}{f_k'}, & \text{if } f_k' > 0 \\ \dfrac{\dot{\underline{q}}_k}{f_k'}, & \text{if } f_k' < 0 \\ \infty, & \text{if } f_k' = 0. \end{cases}$$

Notice that the lower bound on $\dot{u}$ has been posed equal to zero in order to avoid backward movements.

In the same way, joints accelerations fulfill (35) if $\ddot{u}$ belongs to the interval $\ddot{u} \in \bigcap_{k=1}^{n}[\mu_k\ , \lambda_k]$, with

$$\lambda_k = \begin{cases} \dfrac{\ddot{\overline{q}}_k - f_k''\dot{u}^2}{f_k'}, & \text{if } f_k' > 0 \\ \dfrac{\ddot{\underline{q}}_k - f_k''\dot{u}^2}{f_k'}, & \text{if } f_k' < 0 \\ \infty, & \text{if } f_k' = 0 \end{cases}$$

$$\mu_k = \begin{cases} \dfrac{\ddot{\underline{q}}_k - f_k''\dot{u}^2}{f_k'}, & \text{if } f_k' > 0 \\ \dfrac{\ddot{\overline{q}}_k - f_k''\dot{u}^2}{f_k'}, & \text{if } f_k' < 0 \\ -\infty, & \text{if } f_k' = 0 \end{cases}$$

while (36) is satisfied, and $\dddot{u}$ is feasible, if $\dddot{u} \in \bigcap_{k=1}^{n}[\sigma_k\ , \rho_k]$, with

$$\rho_k = \begin{cases} \dfrac{\dddot{\overline{q}}_k - f_k'''\dot{u}^3 - 3f_k''\dot{u}\ddot{u}}{f_k'}, & \text{if } f_k' > 0 \\ \dfrac{\dddot{\underline{q}}_k - f_k'''\dot{u}^3 - 3f_k''\dot{u}\ddot{u}}{f_k'}, & \text{if } f_k' < 0 \\ \infty, & \text{if } f_k' = 0 \end{cases}$$

$$\sigma_k = \begin{cases} \dfrac{\dddot{\underline{q}}_k - f_k'''\dot{u}^3 - 3f_k''\dot{u}\ddot{u}}{f_k'}, & \text{if } f_k' > 0 \\ \dfrac{\dddot{\overline{q}}_k - f_k'''\dot{u}^3 - 3f_k''\dot{u}\ddot{u}}{f_k'}, & \text{if } f_k' < 0 \\ -\infty, & \text{if } f_k' = 0. \end{cases}$$

In conclusion, all kinematic and dynamic constraints are certainly satisfied if, at any time, $\dot{u}$, $\ddot{u}$, and $\dddot{u}$ are bounded between proper intervals. More precisely, $\dot{u}$ is feasible only if it lies in the interval $[R^-,\ R^+]$ where

$$R^- := 0\ , \quad R^+ := \min_{k=1,\ldots,n}\{\eta_k\}\ . \tag{37}$$

Analogously, $\ddot{u}$ is feasible if $\ddot{u} \in [S^-\ , S^+]$, where

$$S^- := \max_{k=1,\ldots,n}\{\beta_k, \mu_k\}\ , \quad S^+ := \min_{k=1,\ldots,n}\{\alpha_k, \lambda_k\} \tag{38}$$

while feasibility of $\dddot{u}$ requires that $\dddot{u} \in [U^-\ , U^+]$, where

$$U^- := \max_{k=1,\ldots,n}\{\delta_k, \sigma_k\}\ , \quad U^+ := \min_{k=1,\ldots,n}\{\gamma_k, \rho_k\}. \tag{39}$$

Configurations such that $R^- > R^+$, $S^- > S^+$, or $U^- > U^+$ could arise. They indicate that, owing to the manipulator current status of motion, *Problem 1* admits no feasible solution; therefore, at least one dynamic or kinematic limit is violated with certainty. It is worth noting that, since such bounds are online evaluated depending on the controller deeds, it is not possible to guarantee *a priori* that a feasible solution exists with certainty.

The fulfillment of the longitudinal bounds is ascribed to a nonlinear trajectory scaling filter whose scheme is shown in Fig. 3. It is composed by two basic elements: a nonlinear algebraic feedback control system that is designed by means of variable structure techniques, followed by a chain of three discrete-time integrators. The nonlinear controller is robustly stable and has been designed to guarantee that output u always tracks, at best and compatibly with assigned limits on $\dot{u}$, $\ddot{u}$, and $\dddot{u}$, a given reference signal u_d, known together with its first and second time derivatives. More precisely, the filter guarantees an output signal u characterized by bounded first, second, and third time derivatives, i.e.,

$$R^- \leq \dot{u} \leq R^+, \quad S^- \leq \ddot{u} \leq S^+, \quad U^- \leq \dddot{u} \leq U^+\ . \tag{40}$$

The bounds which appear in (40) are freely assignable and can be time varying: Changes are also allowed during transients. If (40) are not satisfied because of the filter initial conditions or a sudden bounds change, $\dddot{u}$ is forced within the given limits in a single step, while $\dot{u}$ and $\ddot{u}$ reach the assigned bounds in minimum time. If a discontinuous signal u_d is applied or u_d admits unfeasible time derivatives, its tracking is voluntarily lost. It is achieved again, still in minimum time, as soon as u_d newly becomes feasible. In general, every time a feasible input signal u_d is applied to the filter, tracking condition $u = u_d$ is obtained in minimum time and, compatibly with (40), without overshoot. The filter is similar to that proposed in [23]; therefore, the interested reader can refer to that paper for technical details.

V. Simulation Results

The proposed trajectory scaling technique has been simulated by considering a fictitious RP planar manipulator whose dynamic parameters are reported in Table I. Viscous and Coulomb friction have been modeled as follows:

$$v_i = v_{1i}\,\dot{q}_i + v_{2i}\,\mathrm{sign}(\dot{q}_i)\ , \quad i = 1, 2$$

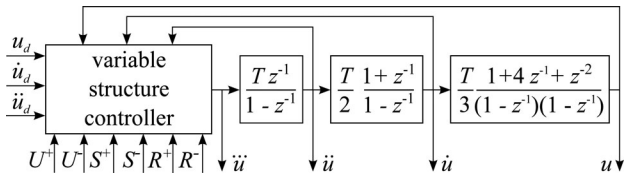

Fig. 3. Detail of the automatic trajectory scaling system composed by a chain of three integrators driven by a variable structure controller.

TABLE I
ROBOT INERTIAL PARAMETERS

Link	Mass	Center of gravity			Inertia		
q	m (Kg)	x(m)	y(m)	z(m)	I_{xx}(Kg m^2)	I_{yy}(Kg m^2)	I_{zz}(Kg m^2)
θ_1	23.90	0	0.10	0	2.521	1.671	1.358
d_2	3.88	0	-0.30	0	0.336	0.336	0.026

where $v_{11} = 1.5\text{e}{-3}$ N·m·s/rd, $v_{21} = 2$ N·m, $v_{12} = 2.8\text{e}{-3}$ N·s/m, and $v_{22} = 2$ N. Controller gains are equal to $\mathbf{k}_p = [800\ 2500]^T$ and $\mathbf{k}_v = [20\ 30]^T$.

The reference path is represented by the following ellipse:

$$\mathbf{f}(u) = \begin{bmatrix} \theta_1 \\ d_2 \end{bmatrix} := \begin{bmatrix} \text{Atan2}(0.8 \sin u, 0.4 \cos u) \\ \sqrt{0.4^2 \cos^2 u + 0.8^2 \sin^2 u} \end{bmatrix} \tag{41}$$

while the following longitudinal time law has been used

$$u_d(t) = \begin{cases} 2\,t^2, & 0 \le t < 0.5 \\ 2t - \dfrac{1}{2}, & 0.5 \le t < 1.5 \\ t - 1, & 1.5 \le t < 3.0 \\ \dfrac{3}{2}t - \dfrac{1}{2}, & 3.0 \le t. \end{cases} \tag{42}$$

Signals $\dot{u}_d(t)$ and $\ddot{u}_d(t)$ are discontinuous; therefore, they do not fulfill the conditions of Proposition 2. GFs are certainly discontinuous; therefore, under the hypothesis of bounded GFDs, path tracking is lost with certainty.

The following bounds for GFs and GFDs have been assumed: $\tau_1, \tau_2 \in [-20, 20]$, $\dot{\tau}_1, \dot{\tau}_2 \in [-300, 300]$. Analogously, joints velocities, accelerations, and jerks have been constrained between the following limits: $\dot{q}_1, \dot{q}_2 \in [-0.8, 2.5]$, $\ddot{q}_1, \ddot{q}_2 \in [-8, 10]$, $\dddot{q}_1, \dddot{q}_2 \in [-110, 180]$. In order to reduce the number of figures, the same bounds have been adopted for the two joints, but in general, such bounds can be arbitrarily selected.

In Section I, it has been pointed out that GFs discontinuity should be avoided. Such discontinuities can be caused, for example, by a longitudinal time law like (42). Let us consider the aforementioned system in which all constraints have been disabled apart from those on GFs. Fig. 4(a) shows the shapes of GFs if reference signal (41), (42) is directly applied to the controller; discontinuities are evident. The maximum tracking error, which is defined as the maximal Euclidean distance between the manipulator tool frame and the reference path, is relevant because of GFs saturations. More precisely, it is equal to 8.557e-3 m. Now, suppose that, in order to reduce such error, the filter that was proposed in [17] is used. GFs assume the shape shown in Fig. 4(b): GF constraints are satisfied so that the worst-case error decreases to 4.698e-4 m, but discontinuities on GFs have been accentuated. In particular, GFs assume a bang–bang behavior in order to guarantee minimum-time transients. In both cases, discontinuities solicit the system and, moreover, if GFD constraints are activated, path tracking is totally lost.

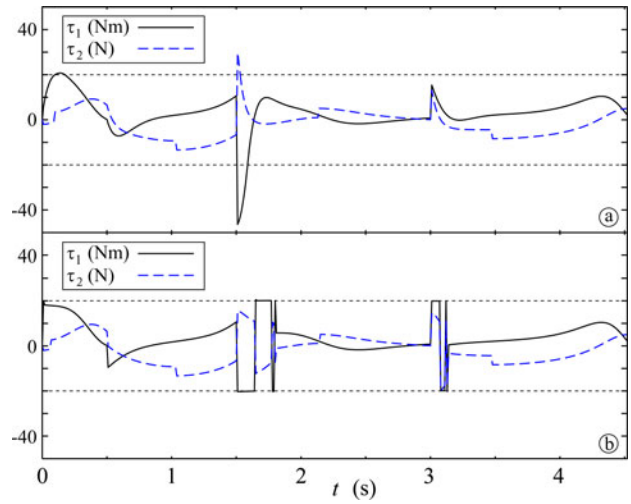

Fig. 4. Output of the IDC that is obtained without (a) or with (b) the filter proposed in [17].

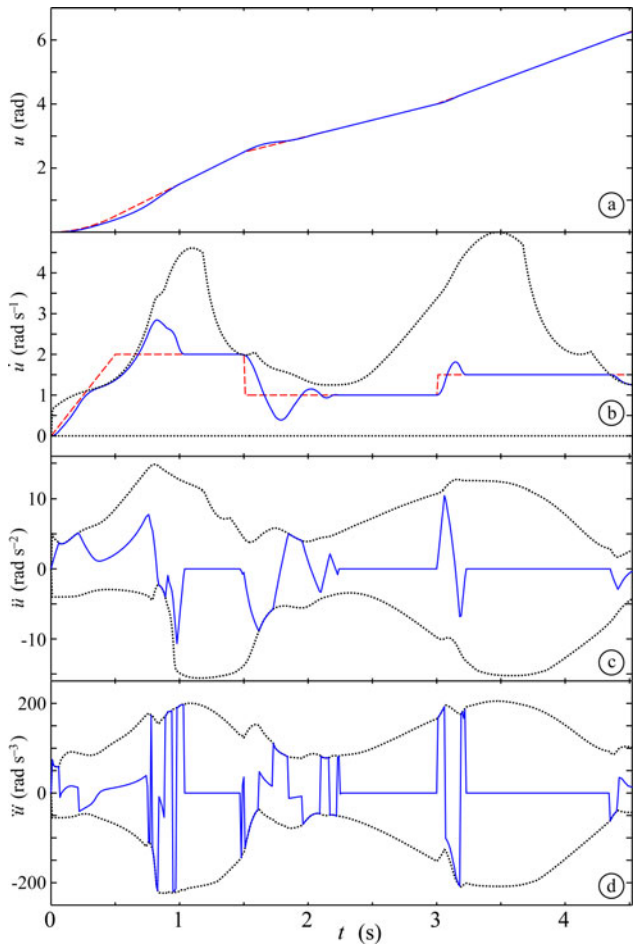

Fig. 5. (a) Position reference signal u_d (dashed line) compared with the filter output u (solid line). (b) Velocity reference signal $\dot{u}_d$ (dashed line) compared with the filter output $\dot{u}$ (solid line) and the velocity bounds (dotted lines). (c) and (d) Online evaluated acceleration and jerks bounds (dotted lines) compared with the filter output $\ddot{u}$ and $\dddot{u}$ (solid lines).

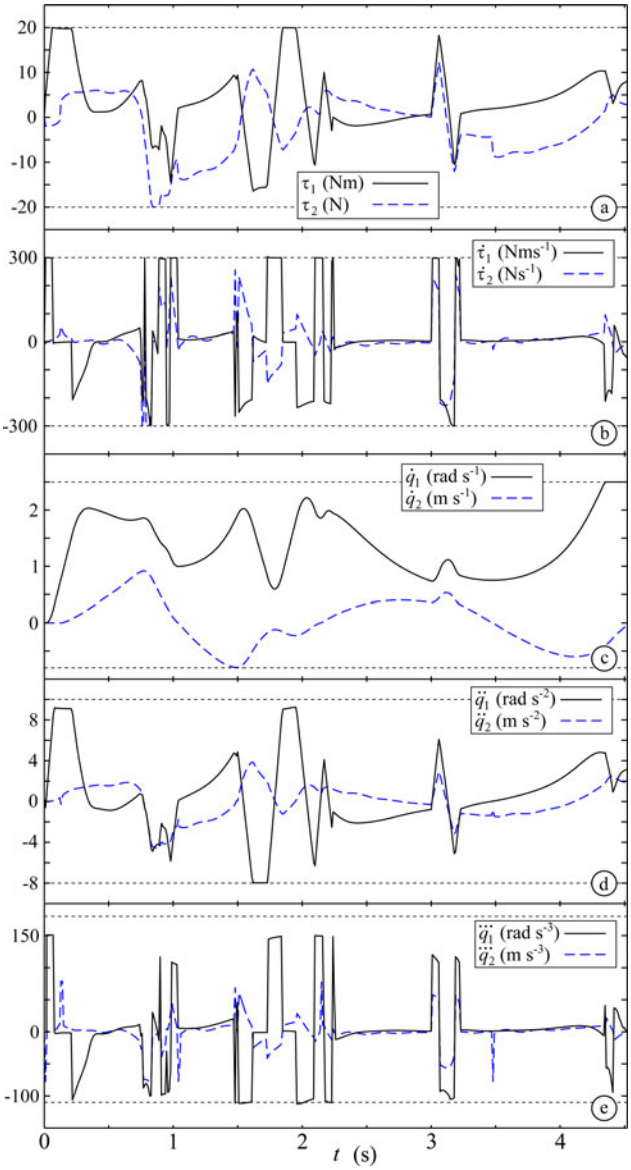

Fig. 6. (a) GFs, (b) GFDs, (c) velocities, (d) accelerations, and (e) jerks for the two joints compared with the given constraints.

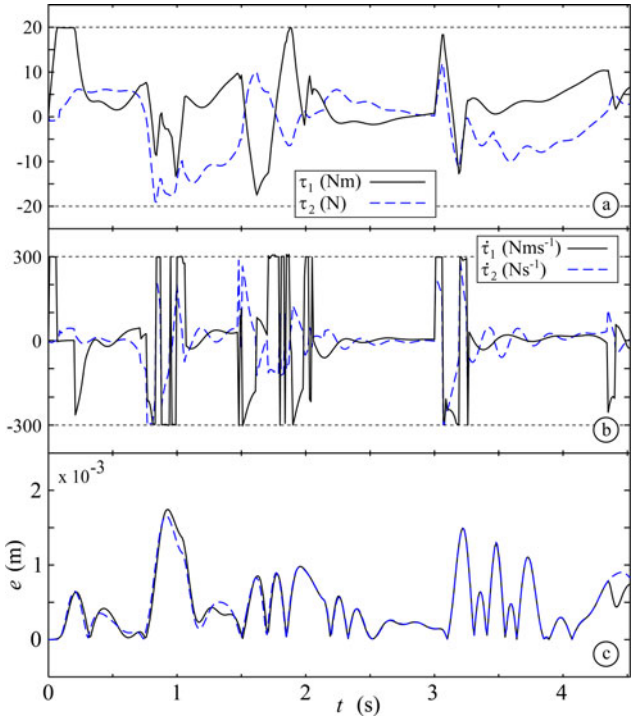

Fig. 7. Simulation results considering an uncertain model. (a) GFs and (b) GFDs for the two joints. (c) Path tracking errors detected by considering model saturations (solid line) or by neglecting them (dashed lines).

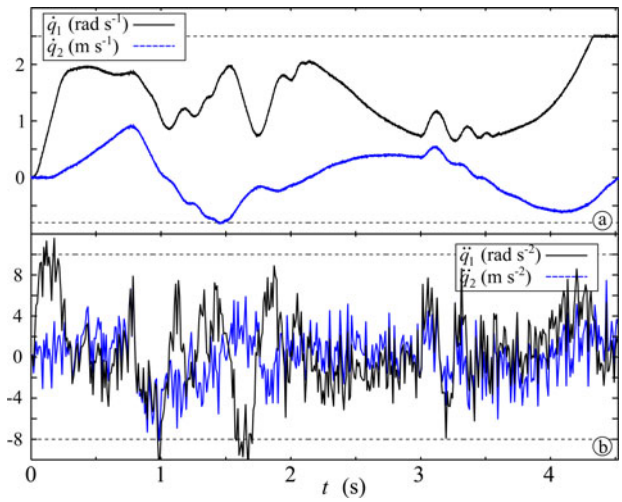

Fig. 8. Effects of measurement noise. (a) Acquired velocities and (b) estimated accelerations compared with the given constraints.

The scaling system proposed in this paper, still guaranteeing minimum-time transients, is able to constrain GFDs between assigned bounds, thus eliminating GF discontinuities and fulfilling possible system constraints on GFDs. In the first simulation, the manipulator model is supposed to be perfectly known. All kinematic and dynamic constraints have been activated. Simulation results are shown in Fig. 5. In particular, Fig. 5(a), which compares u_d (dashed line) with u (solid line), makes it possible to highlight that reference signal u_d is sometime lost to fulfill constraints, but compatibly with the same constraints, the filter continuously attempts to hang $u_d(t)$ in minimum time, thus eliminating tracking delay. Fig. 5(b), (c), and (d) compares signals $\dot{u}$, $\ddot{u}$, and $\dddot{u}$ with the corresponding equivalent kinematic bounds that are evaluated by means of (37)–(39): As desired, equivalent limits are never exceeded. According to the theory, this implies, in turn, that the joints dynamic and kinematic constraints are satisfied, as proved by Fig. 6. It is also evident from the same figure that, as desired, discontinuities on GFs have been eliminated. The maximum tracking error is equal to 5.643e-4 m, i.e., it is similar to that achieved in the first simulation of this section, when the filter proposed in [17] was used. In both cases, constraints are not violated, therefore, such error essentially depends on the IDC tunings.

A further simulation shows the consequences of model uncertainties. Uncertainties affect system performances in several different ways. First, a larger error is obtained because of the poor performances of the IDC. Second, because of this larger error, system outputs saturate more often, further worsening tracking performances. The trajectory scaling system is able to eliminate this latter source of problems, provided that the manipulator model used for the implementation of the

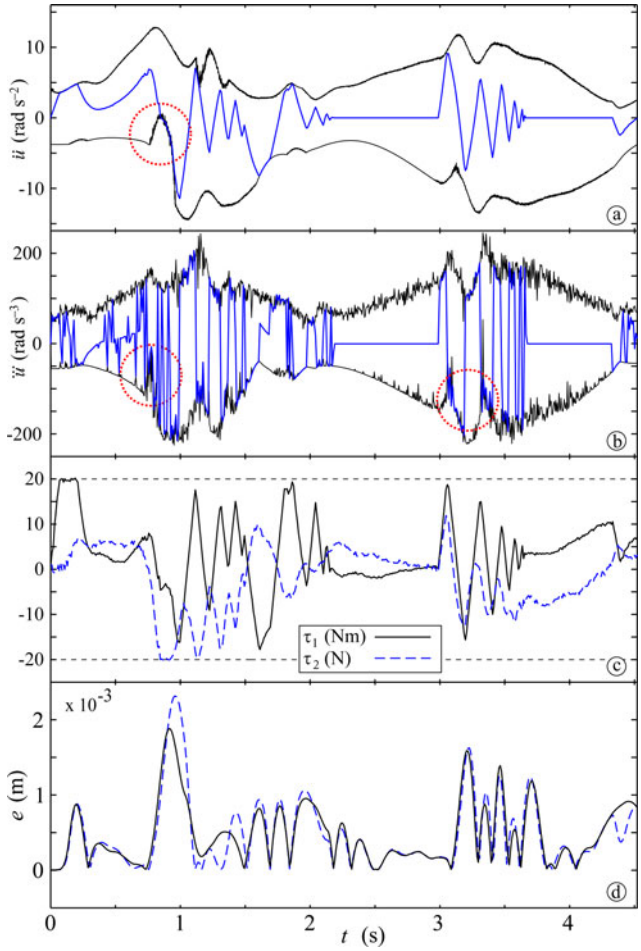

Fig. 9. Effects of measurement noise (a) on $\ddot{u}$ and (b) on $\dddot{u}$ and their equivalent longitudinal bounds; effects on (c) GFs. (d) Path tracking errors detected by considering model saturations (solid line) or by neglecting them (dashed lines).

boundary estimator block is the same adopted for the controller. The online evaluation of bounds (37)–(39) could potentially be the reason of further inaccuracies. Indeed, limits are obtained under the hypothesis that the manipulator perfectly tracks the given path. If path tracking accuracy decreases because of the poor controller performances, equivalent bounds are imprecisely evaluated so that it could happen that they are satisfied, but actual joint constraints are not.

Effects of system uncertainties have been verified by considering a manipulator whose inertia tensors and link masses have been perturbed by 20%. Viscous friction is supposed to be completely unknown, while coulomb friction is underestimated: $v_{21} = 1$ N·m and $v_{22} = 1$ N. As expected, equivalent constraints on the longitudinal time law are still satisfied so that, as shown in Fig. 7(a) and (b), dynamic constraints are fulfilled. Fig. 7(c) shows path tracking errors that are obtained by activating (solid line) or deactivating (dashed line) the model saturations. Differences between the two signals indicate constraints' violations. Only minor differences have been detected: Tracking error is larger with respect to that measured in the ideal case, but since bounds are not violated, it is only caused by the reduced capabilities of the IDC.

The last simulation, still considering an uncertain model, verifies the impact of the acquisition noise. As shown in Fig. 8, a white noise has been added to measured velocities. Accelerations have been evaluated by low-pass filtering velocities and by numerically differentiating the resulting signals. Disturbances could potentially worsen the performances of the scaling system, since they act on equivalent bounds (25), (26), (32), and (33). This is immediately clear from Fig. 9(a) and (b): Equivalent longitudinal bounds become very noisy and change very fast so that the scaling system, owing to its intrinsically limited dynamics, sometimes violates them (see dotted circles). Nevertheless, duration and amplitude of such violations are limited—see the shape of GFs shown in Fig. 9(c)—so that the order of magnitude of tracking errors is similar to that detected without noise. This is proved by Fig. 9(d), which compares, again, errors that are obtained with the saturated and the unsaturated model: Error shapes are different, thus highlighting constraints' violations, but their order of magnitude is the same.

VI. Conclusion

To avoid potential problems that derive from discontinuous GF signals, an online trajectory scaling system has been proposed, which is based on a dynamic filter that automatically modifies reference trajectories in order to fulfill given constraints, thus preserving an accurate path tracking. Simulation results prove that the scaling system is robust with respect to model uncertainties, while acquisition noise has a limited influence on its performances. Only in the case of huge measurement noises, large errors on the equivalent longitudinal bounds have to be expected: This suggests to carefully handle input signals. Nevertheless, the scaling system is perfectly able to work with noisy signals of reasonable amplitude. In particular, simulations have shown that, because of noise, minor constraints' violations can be detected, which have a marginal influence on path tracking errors, and a large chattering appears on the longitudinal jerk. Such chattering does not represent an actual problem since, being the manipulator driven by means of (21), it does not propagate along the control scheme.

References

[1] A. De Luca, L. Lanari, and G. Oriolo, "A sensitivity approach to optimal spline robot trajectories," *Automatica*, vol. 27, no. 3, pp. 535–539, May 1991.

[2] K. Kant and S. Zucker, "Toward efficient trajectory planning: The path-velocity decomposition," *Int. J. Robot. Res.*, vol. 5, no. 3, pp. 72–89, 1986.

[3] J. M. Hollerbach, "Dynamic scaling of manipulator trajectories," *J. Dyn. Sys. Meas. Control*, vol. 106, no. 1, pp. 102–106, 1984.

[4] S. Moon and S. Ahmad, "Time scaling of cooperative multirobot trajectories," *IEEE Trans. Syst. Man Cybern.*, vol. 21, no. 4, pp. 900–908, Jul./Aug. 1991.

[5] A. De Luca and R. Farina, "Dynamic scaling of trajectories for robots with elastic joints," in *Proc. IEEE Int. Conf. Robot. Autom.*, Washington, DC, May 2002, pp. 2436–2442.

[6] K. G. Shin and N. D. McKay, "Minimum-time control of robotic manipulators with geometric path constraints," *IEEE Trans. Automat. Control*, vol. AC-30, no. 6, pp. 531–541, Jun. 1985.

[7] J. E. Bobrow, S. Dubowsky, and J. S. Gibson, "Time-optimal control of robotics manipulators along specified paths," *Int. J. Robot. Res.*, vol. 4, no. 3, pp. 3–17, 1985.

[8] J. Kieffer, A. Cahill, and M. James, "Robust and accurate time-optimal path-tracking control for robot manipulators," *IEEE Trans. Robot. Automat.*, vol. 13, no. 6, pp. 880–890, Dec. 1997.

[9] G. Antonelli, S. Chiaverini, and G. Fusco, "A new on-line algorithm for inverse kinematics of robot manipulators ensuring path tracking capability under joint limits," *IEEE Trans. Robot. Automat.*, vol. 19, no. 1, pp. 162–167, Feb. 2003.

[10] T. Sugie, K. Fujimoto, and Y. Kito, "Obstacle avoidance of manipulators with rate constraints," *IEEE Trans. Robot Automat.*, vol. 19, no. 1, pp. 168–174, Feb. 2003.

[11] O. Dahl and L. Nielsen, "Torque-limited path following by online trajectory time scaling," *IEEE Trans. Robot. Automat.*, vol. 6, no. 5, pp. 554–561, Oct. 1990.

[12] O. Dahl, "Path-constrained robot control with limited torques-experimental evaluation," *IEEE Trans. Robot. Automat.*, vol. 10, no. 5, pp. 658–669, Oct. 1994.

[13] H. Arai, K. Tanie, and S. Tachi, "Path tracking control of a manipulator considering torque saturation," *IEEE Trans. Ind. Electron.*, vol. 41, no. 1, pp. 25–31, Feb. 1994.
[14] M. Kumon, T. Nakata, and N. Adachi, "Biped gait synthesis based on dynamic parametrization," in *Proc. IEEE Int. Conf. Intell. Robots Syst.*, Maui, HI, Oct. 2001, pp. 506–511.
[15] W. Owen, E. A. Croft, and B. Benhabib, "Real-time trajectory resolution for a two-manipulator machining system," *J. Robot. Syst.*, vol. 22, no. S1, pp. S51–S63, Sep. 2006.
[16] J. Moreno-Valenzuela and E. Oronzco-Manríquez, "A new approach to motion control of torque-constrained manipulators by using time-scaling of reference trajectories," *J. Mech. Sci. Technol.*, vol. 23, no. 12, pp. 3221–3231, Dec. 2009.
[17] O. Gerelli and C. Guarino Lo Bianco, "Nonlinear variable structure filter for the online trajectory scaling," *IEEE Trans. Ind. Electron.*, vol. 56, no. 10, pp. 3921–3930, Oct. 2009.
[18] J. Moreno-Valenzuela, "Time-scaling of trajectories for point-to-point robotic tasks," *ISA Trans.*, vol. 45, no. 3, pp. 407–418, Jul. 2006.
[19] D. Constantinescu and E. A. Croft, "Smooth and time-optimal trajectory planning for industrial manipulators along specified paths," *J. Robot. Syst.*, vol. 17, no. 5, pp. 233–249, 2000.
[20] C. Guarino Lo Bianco and A. Piazzi, "Minimum-time trajectory planning of mechanical manipulators under dynamic constraints," *Int. J. Control*, vol. 75, no. 13, pp. 967–980, 2002.
[21] O. Gerelli and C. Guarino Lo Bianco, "Real-time path-tracking control of robotic manipulators with bounded torques and torque-derivatives," in *Proc. 2008 IEEE/RSJ Int. Conf. Intell. Robots Syst.*, Nice, France, Sep. 2008, pp. 532–537.
[22] C. Guarino Lo Bianco and O. Gerelli, "Trajectory scaling for a manipulator inverse dynamics control subject to generalized force derivative constraints," in *Proc. IEEE/RSJ Int. Conf. Intell. Robots Syst.*, St. Louis, MO, Oct. 2009, pp. 5749–5754.
[23] O. Gerelli and C. Guarino Lo Bianco, "A discrete-time filter for the on-line generation of trajectories with bounded velocity, acceleration, and jerk," in *Proc. IEEE Int. Conf. Robot. Autom.*, Anchorage, AK, May 2010, pp. 3989–3994.
[24] C. Guarino Lo Bianco, "Evaluation of generalized force derivatives by means of a recursive Newton-Euler approach," *IEEE Trans. Robot.*, vol. 25, no. 4, pp. 954–959, Aug. 2009.

Sequential Composition for Navigating a Nonholonomic Cart in the Presence of Obstacles

Vinutha Kallem, *Member, IEEE*, Adam T. Komoroski, and Vijay Kumar, *Fellow, IEEE*

***Abstract*—In this study, we consider the problem of safely steering a planar nonholonomic cart around obstacles to reach a goal state. We achieve this by the decomposition of the free workspace into triangular tori and generation of local smooth feedback laws that drive the robot from one cell to an adjoining cell. These control laws exploit the fact that for nonholonomic systems, one can generate smooth controllers to reach a particular subset in the configuration space, even though smooth feedback laws cannot be obtained to reach a particular state. These local controllers are then sequenced using discrete motion planning algorithms like A* or incremental D* to reach the goal. We demonstrate the practical efficacy of this methodology by applying it to two experimental platforms: 1) a differential drive robot in which inertial effects are negligible and 2) a hexapedal robot in which inertial effects are significant but difficult to model. In both cases, we use the abstraction of a planar kinematic cart with process noise to develop feedback controllers. We present successful implementation of the controllers to navigate the hexapedal robot in both static and dynamic environments with obstacles.**

***Index Terms*—Cluttered environments, feedback control, legged robots, mobile robots, motion control.**

I. Introduction

While nonholonomic robots are omnipresent, whether as wheeled robots, legged robots, or as flying robots, their control is often challenging, more so in the presence of obstacles. Brockett [8] showed that nonholonomic systems cannot be steered to a goal position using smooth feedback. This is usually accounted for by using a time-varying controller or by using hybrid controllers [16], [19], [23], [25], [34]. Any real situation typically involves navigation of robots around obstacles, making controller design nontrivial. Potential functions and their gradients have been used by Khatib [17] to navigate fully actuated robots. While this method is simple and avoids obstacles, it has spurious minima that may result in the robot not converging to the actual goal. Rimon and Koditschek [27] develop a class of navigation functions in star worlds that account for the spurious minima and obstacles. Lopes and Koditschek [23] develop a navigation function-based hybrid controller to drive a three-state nonholonomic system to a desired goal location. All these are global controllers that take into account the full information of the environment and the locations of obstacles to design feedback control laws.

In contrast, in sequential composition [9], a set of local feedback controllers are designed and are called upon sequentially. The main idea here is that each local controller prepares the system for the successive

Manuscript received July 17, 2010; revised February 17, 2011; accepted June 26, 2011. Date of publication August 12, 2011; date of current version December 8, 2011. This paper was recommended for publication by Associate Editor T. Simeon and Editor G. Oriolo upon evaluation of the reviewers' comments. This work was supported by the Army Research Office under Grant W911NF-05-1-0219, by the Office of Naval Research under Grant N00014-07-1-0829 and Grant N00014-09-1-1051, and by the Army Research Laboratory under Grant W911NF-10-2-0016 and Grant W911NF-08-2-0004.

The authors are with the Department of Mechanical Engineering and Applied Mechanics, University of Pennsylvania, PA 19104 USA (e-mail: vkallem@seas.upenn.edu; adamtk@seas.upenn.edu; kumar@seas.upenn.edu).

This paper has supplementary downloadable material available at http://ieeexplore.ieee.org.

Color versions of one or more of the figures in this paper are available online at http://ieeexplore.ieee.org.

Digital Object Identifier 10.1109/TRO.2011.2161159